

# SCIENTIFIC REPORTS



OPEN

## Ca<sup>2+</sup> imaging and gene expression profiling of *Lonicera Confusa* in response to calcium-rich environment

Wenwen Jin<sup>1,3</sup>, Yan Long<sup>4</sup>, Chunhua Fu<sup>1</sup>, Libin Zhang<sup>1</sup>, Jun Xiang<sup>3</sup>, Baoshan Wang<sup>2</sup> & Maoteng Li<sup>1,3</sup>

As a medicinal plant widely planted in southwest karst of China, the study of adaptation mechanisms of *Lonicera confusa*, especially to karst calcium-rich environment, can provide important theoretical basis for repairing desertification by genetic engineering. In this study, the Ca<sup>2+</sup> imaging in the leaves of *L. confusa* was explored by LSCM (Laser Scanning Confocal Microscopy) and TEM (Transmission Electron Microscopy), which revealed that the calcium could be transported to gland, epidermal hair and stoma in the leaves of *L. confusa* in high-Ca<sup>2+</sup> environment. In addition, we simulated the growth environment of *L. confusa* and identified DEGs (Differentially Expressed Genes) under different Ca<sup>2+</sup> concentrations by RNA sequencing. Further analysis showed that these DEGs were assigned with some important biological processes. Furthermore, a complex protein-protein interaction network among DEGs in *L. Confusa* was constructed and some important regulatory genes and transcription factors were identified. Taken together, this study displayed the Ca<sup>2+</sup> transport and the accumulation of Ca<sup>2+</sup> channels and pools in *L. Confusa* with high-Ca<sup>2+</sup> treatment. Moreover, RNA sequencing provided a global picture of differential gene expression patterns in *L. Confusa* with high-Ca<sup>2+</sup> treatment, which will help to reveal the molecular mechanism of the adaptation of *L. confusa* to high-Ca<sup>2+</sup> environment in the future.

Currently, ecological deterioration, soil erosion and desertification increase have seriously restricted the development of local economy in karst area of southwestern China. The use of genetic engineering to repair desertification is an important method in vegetation recovery<sup>1</sup>. As one of typical species in southwestern China, the study on the adaptation mechanisms of *Lonicera confusa* to karst environment, especially to karst calcium-rich environment, can provide important theoretical basis for repairing desertification environment by plant genetic engineering.

Calcium ions (Ca<sup>2+</sup>), one of the most abundant metal elements, is available in most soils<sup>2,3</sup>. It is involved in the growth, development and the adaptation to the environment in plants. It is also one of the most important second messenger upon environmental stimulation<sup>4</sup>. Through the cytoplasmic concentration of Ca<sup>2+</sup> cyclical change, plants response to outside stimulation and produce calcium signals. The calcium target protein, such as calmodulin (CaM), calcium dependence protein kinase (CDPKs) and calcineurin B (CBL), pass down the signal to regulate plant growth, development, photosynthesis and stress resistance<sup>5-7</sup>. On the other side, high concentration of Ca<sup>2+</sup> in the cell can cause toxicity<sup>8,9</sup>. Excessive Ca<sup>2+</sup> restricted the growth of many plants in calcareous soils<sup>10</sup>. For instance, high Ca<sup>2+</sup> interfered with various crucial cell processes, including Ca<sup>2+</sup> dependent signaling, phosphate-based energy metabolism and microskelatal dynamics<sup>6,11,12</sup>. Previous studies indicated that plant cells have evolved to possess fine mechanism to adjust free Ca<sup>2+</sup> concentration in the cytoplasm in response to environmental changes, which mainly through the body Ca<sup>2+</sup> transport system, including Ca<sup>2+</sup>-ATPase and

<sup>1</sup>College of Life Science and Technology, Huazhong University of Science and Technology, Wuhan, 430074, China.

<sup>2</sup>College of Life Science, Shandong Normal University, Jinan, 250000, China. <sup>3</sup>Hubei Key Laboratory of Economic Forest Germplasm Improvement and Resources Comprehensive Utilization, Hubei Collaborative Innovation Center for the Characteristic Resources Exploitation of Dabie Mountains, Huanggang Normal University, Huanggang, 438000, China. <sup>4</sup>Institute of Biotechnology, Chinese Academy of Agricultural Sciences, Beijing, 100081, China. Correspondence and requests for materials should be addressed to L.Z. (email: libinzhang@hust.edu.cn) or J.X. (email: swxj@hgnu.edu.cn)

Ca<sup>2+</sup> channels<sup>8,13–18</sup>. For example, some plant cells can actively transport Ca<sup>2+</sup> from the cytosol into the vacuole, endoplasmic reticulum, mitochondria, plastids and cell walls<sup>8,13,15,19–21</sup>, and other plants could accumulate crystalline Ca oxalate and deposit it in the storage parenchyma, bundle sheath cell, epidermal trichomes or chlorenchyma<sup>12,22–24</sup>.

*L. confusa* belongs to the family Caprifoliaceae. As one medicinal plant with ecological value<sup>25–33</sup>, *L. confusa* could adapt to karst calcium-rich area of southwest China<sup>34,35</sup>. Our previous results showed that *L. confusa* could excrete excess Ca salts via stomata and store the excess Ca<sup>2+</sup> in glands and trichomes<sup>34</sup>. However, the underlying molecular mechanisms of *L. confusa* in response to the excess Ca<sup>2+</sup> remain to be solved. The research of the adaptability of *L. confusa* in response to the karst calcium-rich environment will benefit to the exploration of theoretical knowledge and ecological restoration.

In this study, the ultrastructure of mature leaves treated with high or low Ca<sup>2+</sup> was observed by transmission electron microscope (TEM). Moreover, differentially expressed genes (DEGs) are identified under different Ca<sup>2+</sup> concentrations by employing RNA-seq technology and GeneFishing PCR. The results showed that multiple DEGs were related to Ca<sup>2+</sup> transport and accumulation in *L. confusa*. Furthermore, protein-protein interaction network among DEGs identified some important regulatory genes and transcription factors. In summary, the present results provided the groundwork for revealing the molecular mechanism for the adaptation to calcium-rich environment in *L. confusa*.

## Results

**Calcium in soil could be transported to trichomes, glands, and stoma in the leaves of *L. confusa* with higher Ca<sup>2+</sup> treatment.** The mature leaves of *L. confusa* planted in Nongla Karst Experimental Site (108°19'E, 23°29'N) was performed for microwave digestion and flame atomic absorption spectrometry. The results revealed that the average calcium content was about 5.93 mg·g<sup>-1</sup>, which was much higher than that planted in sandstone soil<sup>36</sup>. In order to identify the distribution law of calcium in the leaves of *L. confusa*, the 0, 25, 50, 75, 100 and 125 mg/L gradient concentration of calcium chloride were used for pouring the plant materials, respectively. The leaves with different concentration of external Ca<sup>2+</sup> treatment were labeled with Fluo-3/AM ester and examined under LSCM.

The previous studies indicated that Fluo-3 fluorescence intensity is proportional to the changes of Ca<sup>2+</sup> concentration<sup>37</sup>. The LSCM results in this study revealed that the fluorescent intensity improved with increased external Ca<sup>2+</sup> treatment (Fig. 1A–J), which indicated that the calcium intake in *L. confusa* and calcium concentration in the soil solution are directly related. Therefore, the leaves in high calcium environment may absorb much more calcium than in normal environment. *L. confusa*, as a calcium resistance plants in karst areas, should possess some mechanisms to avoid excessive Ca<sup>2+</sup> in the cytoplasm to affect the normal signal transmission and the formation of the cytoskeleton dynamics process. Further observation showed that the fluorescent intensity was mainly distributed in trichomes (Fig. 1, red arrows), glands (Fig. 1, white arrows) and stoma (Fig. 1, pink arrows). This result indicated that the excess of Ca<sup>2+</sup> absorbed from soil could transport to trichomes, glands, and stoma, which is consistent with our previous results in mature leaves that planted in Nongla Karst Experimental Site<sup>34</sup>. Moreover, the fluorescent intensity further increased with the Ca<sup>2+</sup> treatment time prolonged (Fig. 1G,K,M,O,Q).

The excess of Ca<sup>2+</sup> could transport to trichomes, glands, and stoma, which was also revealed by using the energy-dispersive X-ray spectrometer for chemical component analysis of the leaves of *L. confusa*. The results showed that the Wt% of calcium in epidermal cell, trichomes, glands, stoma and especially in their surrounding cells of *L. confusa* cultivated in calcareous soil was much higher than that cultivated in sandstone soil (Fig. 2A–D,G). Compared with *L. confusa* in sandstone soil, there were 2.81, 2.68, 2.30 and 6.44-fold increase of Wt% in epidermal cell, trichomes, glands, stoma and their surrounding cells of *L. confusa* in calcareous soil. The content of calcium in the different leaf structure was also measured by using linear scanning method and we found that the ROT count of calcium in trichomes part was much higher than that of other parts (Fig. 2F,H). These results again indicated the excess of Ca<sup>2+</sup> absorbed from calcium rich environment could transport to trichomes, glands, and stoma.

**Many calcium channels and pools are found in the leaves of *L. confusa* in high calcium environment.** As mentioned above, the calcium content in leaves of *L. confusa* planted in calcium rich soil was higher than that in calcium poor soil. In order to make clear how the calcium distributed in cells of *L. confusa*, potassium antimonate was used to localize the calcium in cells by using TEM technique. The smaller and fewer calcium antimonate precipitate were observed in the cells of in *L. confusa* treated with lower concentration of Ca<sup>2+</sup> (25 mg/L, Fig. 3A). In contrast, the relatively larger and orderly arranged stored calcium were observed along the cell wall in the materials treated with higher level of Ca<sup>2+</sup> (125 mg/L, Fig. 3B). This result indicated that formation of the common crystalline formation (such as calcium oxalate) arranged across the cell wall was another important mechanism for *L. confusa* to adapt the higher Ca<sup>2+</sup> environment except for three other mechanisms we reported before<sup>34</sup>.

Calcium antimonate can be chelated by EGTA. Therefore, the antimonite-labeled cells near to glands, stoma in low and high Ca<sup>2+</sup> treatment leaves were treated with EGTA. TEM results showed that there are obviously more Ca<sup>2+</sup> pools in the leaves of *L. confusa* treated with higher Ca<sup>2+</sup> for a certain time (Fig. 3D), and fewer Ca<sup>2+</sup> pools in lower Ca<sup>2+</sup> treated materials (Fig. 3C). Very interestingly, we also observed that more calcium ion channels in the *L. confusa* treated with higher Ca<sup>2+</sup> than in lower Ca<sup>2+</sup> treated materials (Fig. 3C,D, arrow heads), which suggested that *L. confusa* could store the Ca<sup>2+</sup> in the calcium pools. Taken together, our results indicated more calcium channels and pools were distributed in the leaves of *L. confusa* in high-Ca<sup>2+</sup> environment than in low-Ca<sup>2+</sup> environment.

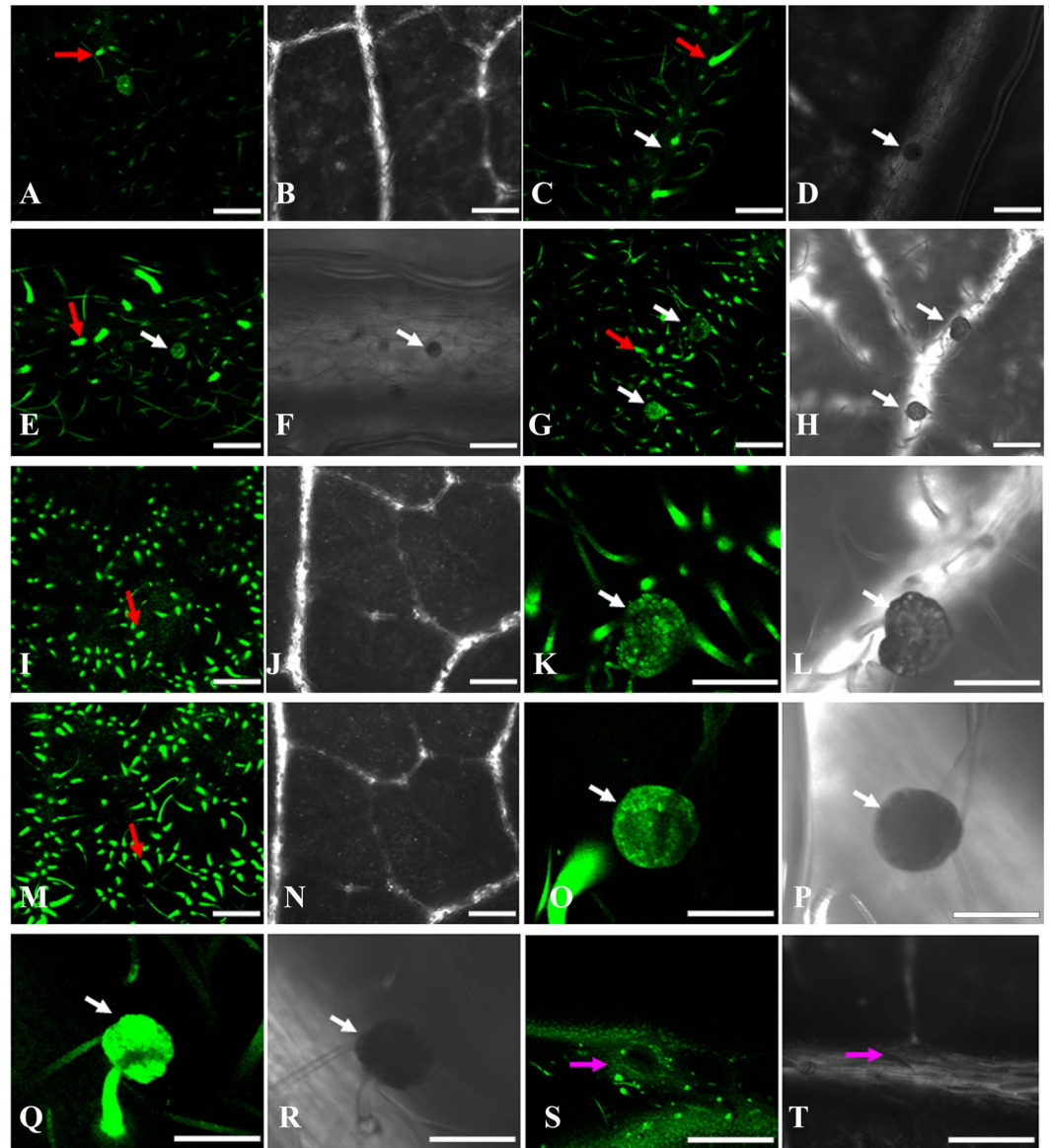


**Figure 1.** Confocal image and the relative density of the fluorescence of *L. confusa* leaves loaded with Fluo-3/AM. (A,C,E,G and I) represent the confocal images of *L. confusa* abaxial surface of leaves after 25, 50, 75, 100 and 125 mg/L  $\text{Ca}^{2+}$  treatment for 36 h. (B,D,F,H and J) represent the perspective images of (A,C,E,G and I), respectively; (K and L) respectively represent the confocal and perspective images of glands after 100 mg/L  $\text{Ca}^{2+}$  treatment for 36 h; (M and N) represent the confocal and perspective images of abaxial surface of leaves after 100 mg/L  $\text{Ca}^{2+}$  treatment for 72 h; (O and Q) represent the confocal images of glands in leaves after 100 mg/L  $\text{Ca}^{2+}$  treatment for 72 h; (P and R) represent the perspective images of glands in leaves after 100 mg/L  $\text{Ca}^{2+}$  treatment for 72 h; (S and T) represent the confocal and perspective images of stomata in the leaves after 100 mg/L  $\text{Ca}^{2+}$  treatment for 72 h. Bar = 100  $\mu\text{m}$ .

**Identification of differentially expressed genes by RNA sequencing in higher and lower calcium-treated *L. confusa*.** The *L. confusa* treated with 125 mg/L calcium chloride solution and pure water (as control) for 24 hours and 30 days were used for DEG analysis. Two biological replicates of RNA-seq of *L. confusa* leaf tissues treated with different level of  $\text{Ca}^{2+}$  were performed. The two sets of the corresponding sequencing samples were combined, which generated 57393938, 69001767 and 60782634 clean reads, respectively. The obtained clean reads were then mapped to the assembled transcriptome of *L. confusa*<sup>38</sup>. The results showed that 35584241, 44851148 and 38596972 clean reads can be mapped to the assembled unigenes<sup>38</sup>, respectively. Among the mapped reads, 24908968, 32292826 and 28171538 clean reads were uniquely mapped to the unigenes, respectively. 10675273, 12558322 and 10425434 clean reads were mapped to multiple locations of unigenes, respectively. After mapping, 94607, 90574 and 86396 expressed unigenes for 0 h, 24-hour and 30-day  $\text{Ca}^{2+}$ -treatment were obtained, respectively. To identify the DEGs between control and calcium-treated *L. Confusa*, we set the expression level of unigenes of control as a control and investigated the up- or down-regulated

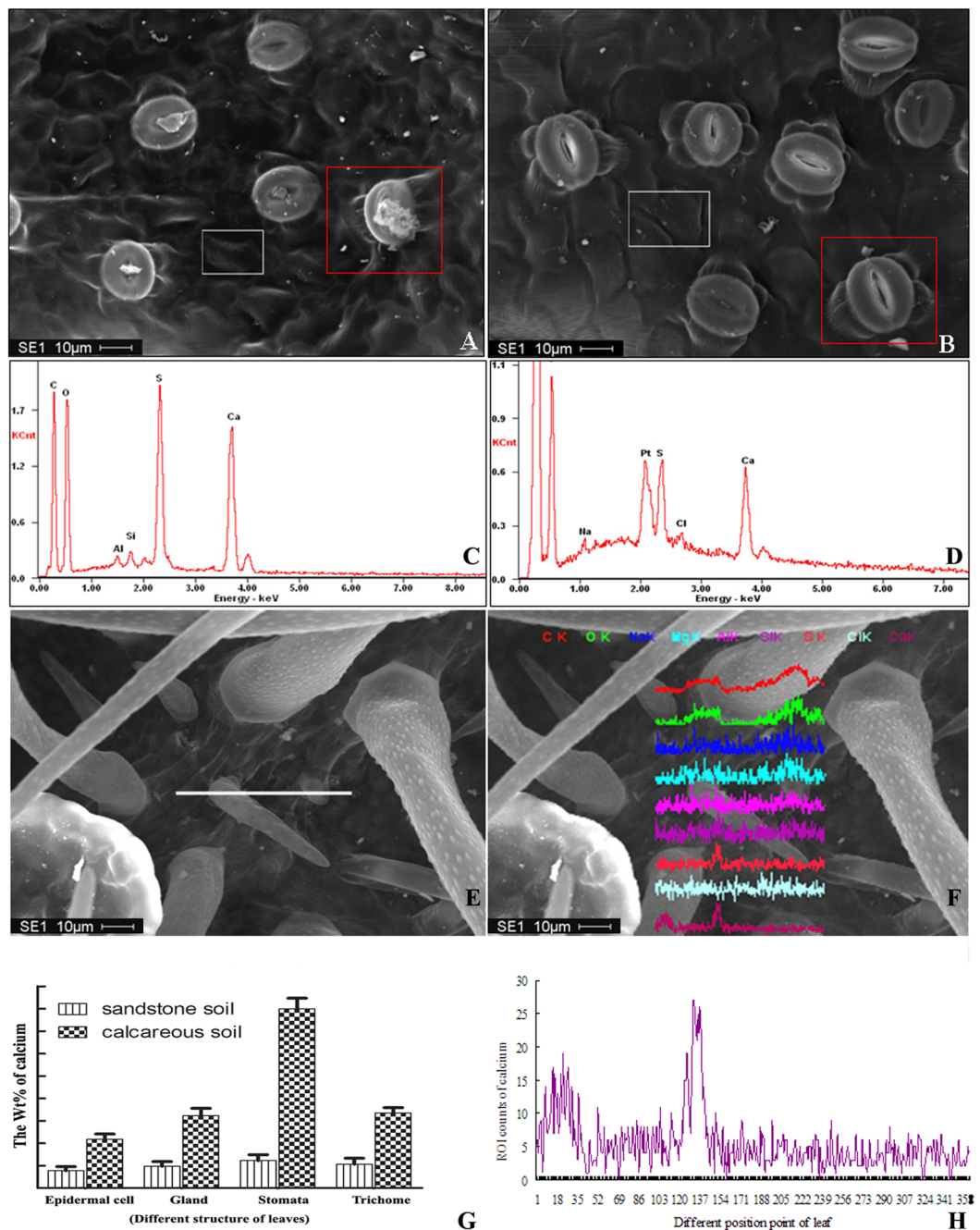


**Figure 2.** The calcium content analysis by using EDX. (A and B) represent the SEM (Scanning Electron Microscopy) map of leaves cultivated in calcareous and sandstone soil (white and red square frames represent the map scanning area of epidermal cells, stomata and its surround cells); (C and D) represent the EDX map of calcium; (E and F) represent the linear scanning area and the different element change in different scanning point (the different color curve represent different element); (G) The Wt % of calcium in different structures cultivated in calcareous and sandstone soil. (H) The amplified calcium change curve in different scanning point from (D).

unigenes of calcium-treated *L. confusa*. The analysis showed that 322,69 unigenes were differentially expressed between control and 24-hour calcium-treatment *L. confusa*, and 43,148 unigenes were differentially expressed between control and 30-day calcium-treatment *L. confusa*. Also, we observed that a total of 34,155 unigenes were differentially expressed between 24-hour and 30-day calcium-treatment *L. confusa* samples, which indicated that short-term (24-hour) and long-term (30-day)  $\text{Ca}^{2+}$  treatment to *L. confusa* may induce different physiological status of *L. confusa*. As shown in Supplementary Fig. 1, these DEGs between control and calcium-treated *L. Confusa* were further annotated with GO terms. Furthermore, the GO-enriched DEGs between control and calcium-treated *L. Confusa* were displayed by heatmap analysis (Fig. 4A). We next performed GeneFishing PCR

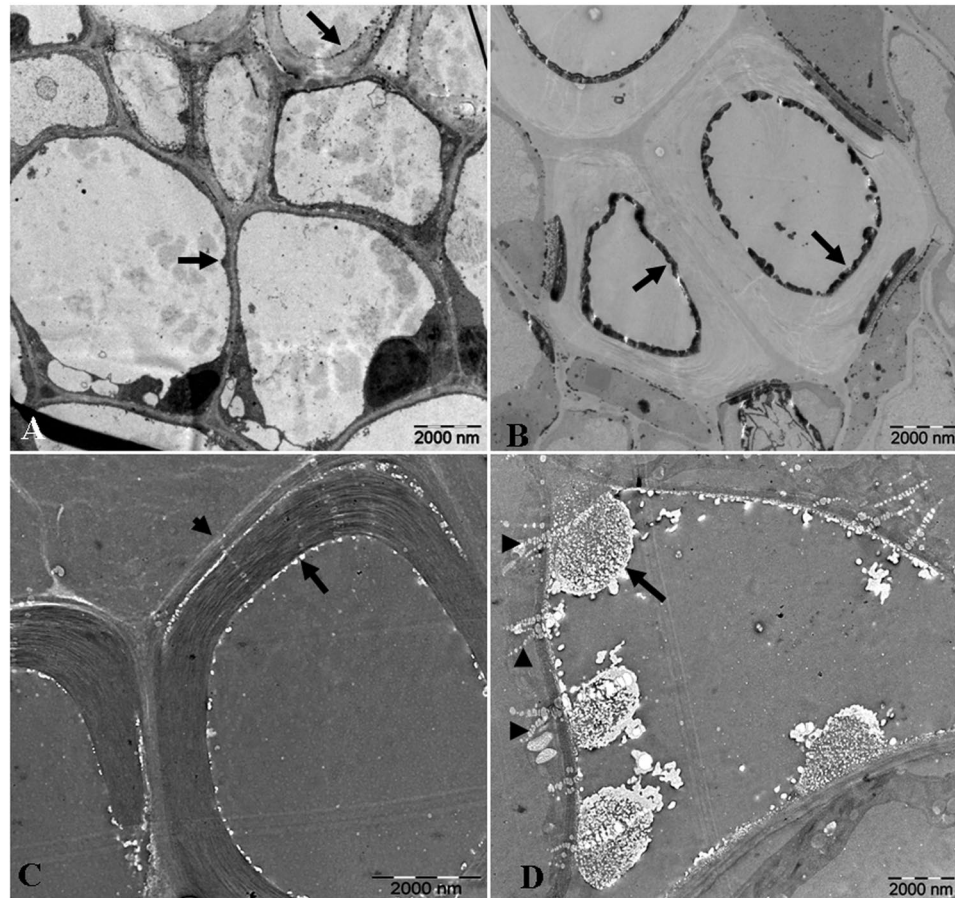


**Figure 3.** TEM analysis of *L. confusa* leaves with high and low  $\text{Ca}^{2+}$  treatment. (A and B) represent TEM analysis of antimonite-labeled cells located in white square frames in Fig. 2b (low  $\text{Ca}^{2+}$  treatment, 25 mg/L) and Fig. 2a (high  $\text{Ca}^{2+}$  treatment, 125 mg/L), respectively (Arrow indicates the calcium antimonate precipitate), (C and D) represent the TEM analysis of antimonite-labeled cells near to glands, stoma in low and high  $\text{Ca}^{2+}$  treatment leaves, respectively. The antimonite-labeled cells were treated with EGTA and the calcium antimonate precipitates were chelated (Arrows indicate the calcium pools and arrow heads indicate the calcium channels).

to validate the DEGs identified in RNA sequencing analysis. The *L. confusa* treated with 125 mg/L calcium chloride solution and pure water (as control) for 30 days were used for GeneFishing analysis. In all, 24 DEGs were identified between control and high  $\text{Ca}^{2+}$ -treated *L. confusa* (Supplementary Table 1). The DEGs were further confirmed by semi-quantitative RT-PCR experiments (Supplementary Fig. 2), which was very consistent with the RNA sequencing results.

Furthermore, Cytoscape software<sup>39</sup> was used to construct a complex protein-protein interaction network among DEGs in *L. confusa*. As shown in Fig. 4B, there were 253 nodes and 762 edges obtained in the network. Some important transcription factors, such as MYB59, WRKY19, WRKY51 and WRKY70 were involved in the network. Also, Tua3 (alpha-3 tubulin), one of the important cytoskeleton components, interacts with 9 targets including EB1C, EB1A, EB1B, ZWI, EMB2804, KIS and so on, in which all target proteins are associated with the formation and biological functions of microtubule. Therefore, the results indicate that Tua3 and target proteins may form a complex network to regulate cell morphology and intercellular transportation *L. confusa*.

**Functional Enrichment of differentially expressed genes.** For functional annotation of DEGs of short-term and long-term  $\text{Ca}^{2+}$  induction *L. confusa*, the DEGs were further analyzed using Cytoscape EnrichmentMap (<http://www.cytoscape.org/>). As shown in Fig. 5, EnrichmentMap analysis of short-term and long-term  $\text{Ca}^{2+}$  induction DEGs generated 300 and 404 nodes, respectively. These nodes were classified into different categories. The common terms between short-term (24 hours) (Fig. 5A) and long-term (30 days) (Fig. 5B)  $\text{Ca}^{2+}$  induction DEGs were “Response to stimulus”, “Developmental process”, “Biological regulation”, “Metabolic process”, “Cellular process” and “Transport”. Very importantly, some DEGs were enriched in different categories. For example, EnrichmentMap analysis showed that short-term  $\text{Ca}^{2+}$  induction DEGs were also clustered in “Signaling”. This result indicated that short-term  $\text{Ca}^{2+}$  induction in *L. confusa* might activate some important signal transduction pathways and/or defense responses. Nevertheless, long-term  $\text{Ca}^{2+}$  induction DEGs were mainly clustered in “Cellular cation homeostasis”, “Component organization” and “Localization”. Interestingly, the enrichment of “Cellular cation homeostasis” suggested that *L. confusa* gradually adapted to high-  $\text{Ca}^{2+}$  environment and kept a new cation balance after long-term  $\text{Ca}^{2+}$  treatment. Meanwhile, “Transport” process was

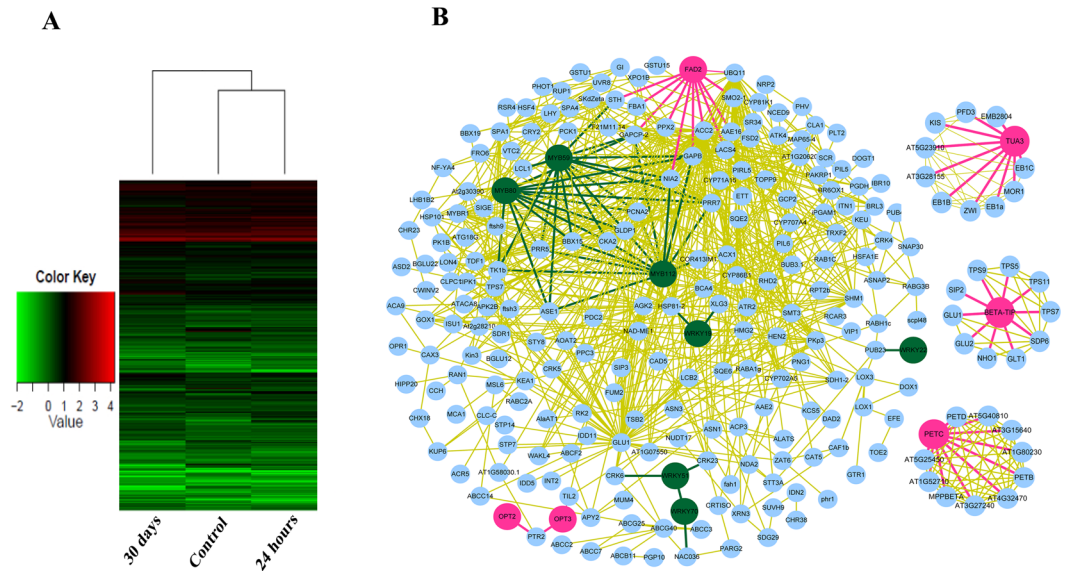


**Figure 4.** (A) Heatmap analysis of differentially expressed genes among control (no  $\text{Ca}^{2+}$  treatment), 24-hour  $\text{Ca}^{2+}$  treatment and 30-day  $\text{Ca}^{2+}$  treatment *L. Confusa*. (B) Protein-protein interaction network of differentially expressed genes in *L. Confusa* constructed by Cytoscape software. Red circles indicate the differentially expressed genes identified in Genefishing experiments. Green circles indicate the identified transcription factors.

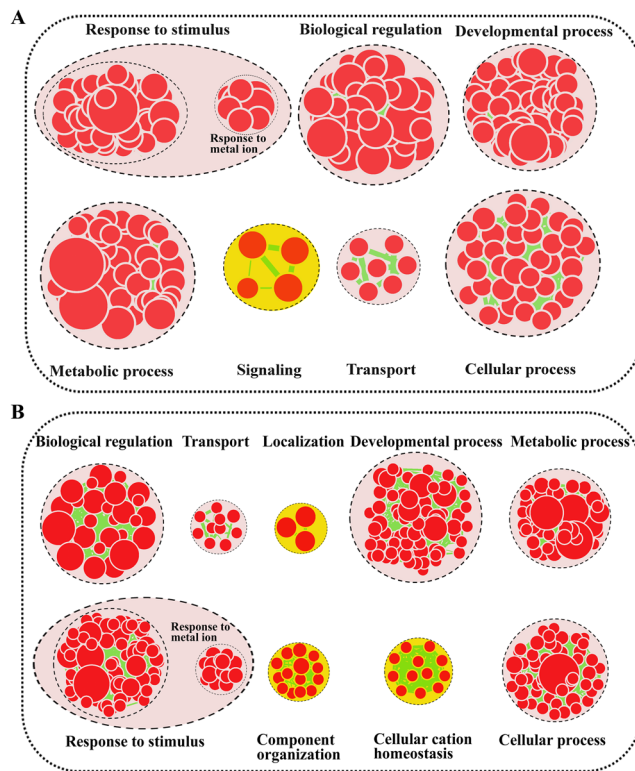


**Figure 5.** Biological Process analysis of differentially expressed genes (DEGs) between short-term (24 hours)  $\text{Ca}^{2+}$  -treated and long-term  $\text{Ca}^{2+}$  treated *L. confusa*. GO modules enriched with short-term (24 hours)  $\text{Ca}^{2+}$  -treated DEGs (A) and long-term (30 days)  $\text{Ca}^{2+}$  treated DEGs (B) were visualized by the EnrichmentMap in Cytoscape. The red and yellow circles indicate the common and different biological processes between short-term (24 hours)  $\text{Ca}^{2+}$  -treated and long-term  $\text{Ca}^{2+}$  -treated *L. confusa*, respectively.

enriched both in short-term and long-term  $\text{Ca}^{2+}$  induction *L. Confusa*, which suggested that  $\text{Ca}^{2+}$  treatment induced the activation of relative  $\text{Ca}^{2+}$  transport pathways in *L. Confusa*.

**KEGG pathway analysis.** To reveal biological functions of the identified genes, the DEGs between control (no  $\text{Ca}^{2+}$  treatment) and 30-day  $\text{Ca}^{2+}$  treatment *L. Confusa* were further assigned for KEGG pathway analysis. As shown in Supplementary Dataset 1, a total of 99 KEGG pathways were ranked by p-value. The top 5 pathways included “Ribosome” (91 unigenes,  $P = 3.97 \times 10^{-7}$ ), “Phenylpropanoid biosynthesis” (61 unigenes,  $P = 1.74 \times 10^{-6}$ ), “Methane metabolism” ( $P = 2.39 \times 10^{-6}$ ), “Cyanoamino acid metabolism” (29 unigenes,  $P = 3.46 \times 10^{-5}$ ) and “Phenylalanine metabolism” (50 unigenes,  $P = 7.06 \times 10^{-5}$ ). Furthermore, we extracted the  $\text{Ca}^{2+}$  metabolism-related pathways for analysis. As shown in Supplementary Fig. 3, the  $\text{Ca}^{2+}$  metabolism-related pathways were classified into five categories including Cellular Processes, Environmental Information Processing, Genetic Information Processing, Metabolism and Organismal Systems. Among them, Cellular Processes category enriched 142 genes in which 32 genes are involved in the pathway of “Transport and catabolism”. More importantly, we observed that a lot of (265) genes are involved in “Signal transduction” pathway in Environmental Information Processing category. These results indicated long-term  $\text{Ca}^{2+}$  treatment on *L. Confusa* may induce  $\text{Ca}^{2+}$  transport and related signal transduction processes.

## Discussion

*L. confusa* is a woody perennial, evergreen and twining vine. It is widely cultivated in eastern Asia as an important medicinal plant. *L. confusa* is also processed into food and a healthy beverage, which facilitates the rapid increase of its commercial value in herbal medicine markets. However, the economy development has been greatly impeded by ecological deterioration, soil erosion and desertification in karst area of southwestern China. *L. confusa* is one of typical species in southwestern China. Therefore, this study focused on the adaptation mechanism of *L. confusa* to karst calcium-rich environment, which will reveal important theoretical basis for repairing desertification environment.

Various studies have revealed that  $\text{Ca}^{2+}$  will accumulate to a very high level over time in cells when water evaporates from the surface of plants. Moreover, the excess  $\text{Ca}^{2+}$  can be precipitated as inactive Ca oxalate<sup>22</sup>. Within plants, most long-distance  $\text{Ca}^{2+}$  transports through plant tissues have been demonstrated to follow apoplastic pathways<sup>40,41</sup>. After the  $\text{Ca}^{2+}$  transfer to the plant cell,  $\text{Ca}^{2+}$  can be transported from the cytosol into the vacuole, endoplasmic reticulum, mitochondria, plastids and cell walls where  $\text{Ca}^{2+}$  can be captured by  $\text{H}^+/\text{Ca}^{2+}$  antiporters (CAX) and  $\text{Ca}^{2+}$ -ATPases (ACA)<sup>8,21</sup>. CAX1 has a primary role in  $\text{Ca}^{2+}$  accumulation in the leaf mesophyll and it is important in controlling apoplastic  $\text{Ca}^{2+}$ , stomatal aperture, and growth<sup>41,42</sup>. In this study, we also observed high- $\text{Ca}^{2+}$  treatment induced the transport of  $\text{Ca}^{2+}$  to trichomes, glands, and stoma in the leaves of *L. Confusa*. Moreover, more calcium channels and calcium pool are accumulated in the leaves of *L. confusa* in high calcium environment. Although the signaling role of  $\text{Ca}^{2+}$  in organisms has developed rapidly<sup>3,21</sup>, fundamental information regarding the mechanisms that regulate  $\text{Ca}^{2+}$  transport and storage in plants still remains elusive<sup>43</sup>.

RNA-seq technology is an effective transcriptome analysis tool, which can detect novel and rare RNA transcripts and accurately quantify gene expression level. In this study, we identified multiple DEGs (differentially expressed genes) between control and calcium-treated *L. Confusa*. Bioinformatics analysis showed that 322,69 unigenes were differentially expressed between control and 24-hour calcium-treatment *L. confusa*, and 43,148 unigenes were differentially expressed between control and 30-day calcium-treatment *L. confusa*. Importantly, the different gene expression level between 0-hour and 24-hour or 30-day  $\text{Ca}^{2+}$ -treated *L. confusa* might be induced not only by the  $\text{Ca}^{2+}$  treatment but also by own natural growth of *L. confusa*. Therefore, we could not fully exclude the effect of 24-hour or 30-day natural growth of *L. confusa* on the gene expression level. Nevertheless, the samples used for RNA-seq were mature leaves of *L. confusa*. We supposed that the gene expression level in the mature leaves is very stable in 24 hours or 30 days, and the different gene expression level between 0-hour and 24-hour or 30-day  $\text{Ca}^{2+}$ -treated *L. confusa* were mainly induced by  $\text{Ca}^{2+}$  treatment. Furthermore, the identified DEGs were validated by GeneFishing PCR. For example, *Tua3*, *CaM*, *CDPKs*, *CBL* and some other important genes were identified. *Tua3* is one of the important cytoskeleton components. Our network analysis showed that *Tua3* interacts with 9 target genes, in which all target genes are associated with the formation of microtubule. Taken together, these results indicate that *Tua3* and target genes may regulate cell morphology and intercellular transportation by a complex gene interaction network in *L. confusa*. In the meanwhile, it has been reported that *CaM*, *CDPKs* and *CBL* are involved in cytoskeleton formation and movement, osmotic stress resistance<sup>44,45</sup>. Calcium, as the second messenger upon environmental stimulation in plant, plays critical roles in response to outside signals and activates the expression of related genes. For  $\text{Ca}^{2+}$  transport into the vacuole in plant cells, both  $\text{Ca}^{2+}$ -ATPases (ACA) and  $\text{Ca}^{2+}/\text{H}^+$  antiporters (CAX) play important roles<sup>46</sup>. Therefore, transcript abundance of transporters could be up-regulated under conditions of adequate Ca supply. Also, proteins that modify activity of transporters, such as *CAM* or *CXIP*, could also be regulated in a similar fashion<sup>47,48</sup>. For instance, compared with epidermal cells, mesophyll cells of *Arabidopsis* have the higher capacity to store  $\text{Ca}^{2+}$  in their vacuoles by virtue of the higher expression of the  $\text{Ca}^{2+}/\text{H}^+$  antiporter on the tonoplast membrane<sup>41</sup>. Our DEGs analysis in this study showed that *CaM* and *CAX* were upregulated in long-term  $\text{Ca}^{2+}$  treated *L. Confusa*, which might reflect the adaptive changes of *L. Confusa* to high- $\text{Ca}^{2+}$  environment. In addition, EnrichmentMap analysis showed that multiple DEGs were involved in “Cellular cation homeostasis” and “Transport” processes. The results suggested that  $\text{Ca}^{2+}$  treatment induced the activation of relative  $\text{Ca}^{2+}$  transport pathways and *L. confusa* gradually adapted to high- $\text{Ca}^{2+}$  environment and kept a new cation balance after long-term  $\text{Ca}^{2+}$  treatment, which is very consistent with our LSCM and TEM results. Collectively, identification of these important DEGs will help us to explore the possible regulatory mechanism of the adaptation to high- $\text{Ca}^{2+}$  environment in *L. confusa*.

## Materials and Methods

**Plant materials.** *L. confusa* cultivars were taken from typical Nongla Karst Experimental Site (108°19'E, 23°29'N) as previously described<sup>34</sup>. The *L. confusa* cultivars were planted in the soils transported from Nongla Karst Experimental Site. In order to remove the calcium ions in the soils, the soils were washed with pure water for several times. Furthermore, 24 basin of *L. confusa* materials were divided into six groups and treated with different concentrations of Ca<sup>2+</sup>, respectively.

**Detection of Ca<sup>2+</sup> on the leaves of *L. confusa* by LSCM.** The Ca<sup>2+</sup> images in the leaves of *L. confusa* were detected as previously described<sup>34,49</sup>. The *L. confusa* leaves growing in soils with different level Ca<sup>2+</sup> were soaked in Fluo-3/AM ester solution at 4 °C for 2 h. These *L. confusa* leaves were then washed with PBS solutions and observed under Olympus FV1000 LSCM (OLYMPUS, JAPAN).

**TEM analysis.** TEM analysis of the leaves of *L. confusa* was performed as previously described<sup>34,50</sup> except for small modification. First, 5 independent leaf samples of *L. confusa* with different level Ca<sup>2+</sup> treatment were isolated, washed with phosphate buffer solution and cut into 0.2 cm × 0.2 cm slices. Furthermore, these samples were fixed and dehydrated through graded ethanol concentrations once for 10 min and soaked in 100% acetone twice for 30 min. Subsequently, the samples were treated with 2% potassium pyroantimonate and dehydrated. Finally, the samples were embedded with Spurr epoxy resin and sectioned with superfine section machine. The obtained sections were dyed and examined using TEM (Dutch FEI Tecnai F20-Twin, Netherlands).

**RNA isolation and GeneFishing PCR.** The total RNA isolation of the *L. confusa* leaves treated with different level of Ca<sup>2+</sup> was performed as previously described<sup>51</sup>. GeneFishing kit (Seegene, Inc.) was used for differential display PCR analysis. GeneFishing<sup>TM</sup> PCR were done with dT-ACP2 and 20 pairs of random primers, the PCR products were run on 2% agarose gel and the cDNA bands ranged from 100 and 1.5 kb were used for cloning and sequencing (Supplementary Fig. 2). QIAquick Gel extraction kit (Qiagen) was used to isolate the differentially expressed bands. The isolated DNA fragments were cloned into pGEM<sup>®</sup>-T Easy vector (Promega) and sequenced. Further Semi-quantitative RT-PCR experiments were utilized for the validation of the GeneFishing results. The Primers used for GeneFishing PCR and Semi-quantitative RT-PCR were shown in Supplementary Tables 2 and 3, respectively.

**RNA sequencing and DEG analysis.** The RNA-seq cDNA libraries of *L. confusa* leaves treated with different level of Ca<sup>2+</sup> were constructed using TruSeq<sup>TM</sup> RNA Sample Preparation Kit (Illumina, Inc.). Shortly, oligo (dT) magnetic beads (NEB) were used to capture poly-A mRNAs from the isolated total RNA. The captured mRNAs were fragmented into 200–500 bp for cDNA synthesis and adaptor ligations. The synthesized cDNAs were PCR-amplified, quantified and sequenced on Illumina HiSeq 2000 using 2 × 100 bp pair-end sequencing protocol. The generated clean reads were deposited in NCBI Sequence Read Archive (SRA) Sequence Database (Accession number: SRR6024635). Bioinformatics analysis of differentially expressed genes of RNA-seq samples was performed as described<sup>37</sup>. Briefly, gene expression level of each RNA-seq sample was measured by RPKM (Reads Per kb per Million reads). The genes with RPKM ≥ 1 were regarded to be expressed in the RNA-seq analysis. The edgeR software was then used to identify the differentially expressed genes. The differentially expressed genes among *L. confusa* leaves treated with different level of Ca<sup>2+</sup> were selected using a log FC (log-fold expression change) > 2 or < -2, a false discovery rate (FDR < 0.001) and p-value < 0.005 as the threshold value.

**Pathway analysis and interaction analysis.** The functions of the DEGs were analyzed by using Kyoto Encyclopedia of Genes and Genomes (KEGG) database (<http://www.genome.jp/tools/blast>). Cytoscape<sub>2\_6\_3</sub> (<http://www.cytoscape.org/plugins/index.php>) was used to analyze the protein-protein interaction among DEGs.

**Accession number.** RNA sequencing data have been deposited in NCBI Sequence Read Archive (SRA) Sequence Database with accession number SRR6024635.

## References

- Hueso-González, P., Martínez-Murillo, J. F. & Ruiz-Sinoga, J. D. Benefits of adding forestry clearance residues for the soil and vegetation of a Mediterranean mountain forest. *Sci Total Environ* **615**, 796–804 (2018).
- Barker, A. & Pilbeam, D. Handbook of plant nutrition. CRC Press, Taylor & Francis Group, Boca Raton (2006).
- Tang, R. J. & Luan, S. Regulation of calcium and magnesium homeostasis in plants: from transporter to signaling network. *Curr Opin Plant Biol* **39**, 97–105 (2017).
- Bartels, D. & Sunekar, R. Drought and salt tolerance in plants. *Crit Rev Plant Sci* **24**, 23–58 (2005).
- Hepler, P. K. Calcium: a central regulator of plant growth and development. *Plant Cell* **17**, 2142–2155 (2005).
- Toyota, M. *et al.* Cytoplasmic calcium increases in response to changes in the gravity vector in hypocotyls and petioles of *Arabidopsis* seedlings. *Plant Physiol* **146**, 505–514 (2008).
- Gao, Q. F. *et al.* Cyclic nucleotide-gated channel 18 is an essential Ca<sup>2+</sup> channel in pollen tube tips for pollen tube guidance to ovules in *Arabidopsis*. *Proc Natl Acad Sci USA* **113**, 3096–3101 (2016).
- Volk, G. M., Goss, L. J. & Franceschi, V. R. Calcium channels are involved in calcium oxalate crystal formation in specialized cells of *Pistia stratiotes* L. *Ann Bot* **93**, 741–753 (2004).
- Harada, E. & Choi, Y. Investigation of metal exudates from tobacco glandular trichomes under heavy metal stresses using a variable pressure scanning electron microscopy system. *Plant Biotechnology* **25**, 407–411 (2008).
- White, P. J. & Broadley, M. R. Calcium in plants. *Ann Bot* **92**, 487–511 (2003).
- Sakano, K. Metabolic regulation of pH in plant cells: role of cytoplasmic pH in defense reaction and secondary metabolism. *Int Rev Cytol* **206**, 1–44 (2001).
- Webb, M. A. Cell-mediated crystallization of calcium oxalate in plants. *Plant Cell* **11**, 751–761 (1999).
- Bush, D. S. Regulation of Cytosolic Calcium in Plants. *Plant Physiol* **103**, 7–13 (1993).
- Hetherington, A. M. & Brownlee, C. The generation of Ca<sup>(2+)</sup> signals in plants. *Annu Rev Plant Biol* **55**, 401–427 (2004).



15. Pittman, J. K. & Hirschi, K. D. Don't shoot the (second) messenger: endomembrane transporters and binding proteins modulate cytosolic Ca<sup>2+</sup> levels. *Curr Opin Plant Biol* **6**, 257–262 (2003).
16. Hou, C. *et al.* DUF221 proteins are a family of osmosensitive calcium-permeable cation channels conserved across eukaryotes. *Cell Res* **24**, 632–635 (2014).
17. Yuan, F. *et al.* OSCA1 mediates osmotic-stress-evoked Ca<sup>2+</sup> increases vital for osmosensing in *Arabidopsis*. *Nature* **514**, 367–371 (2014).
18. Kiepp, V. *et al.* Systemic cytosolic Ca<sup>2+</sup> elevation is activated upon wounding and herbivory in *Arabidopsis*. *New Phytol* **207**, 996–1004 (2015).
19. Harper, J. F. Dissecting calcium oscillators in plant cells. *Trends Plant Sci* **6**, 395–397 (2001).
20. Ge, L. L., Tian, H. Q. & Russell, S. D. Calcium function and distribution during fertilization in angiosperms. *Am J Bot* **94**, 1046–1060 (2007).
21. Choi, W. G. *et al.* Rapid, long-distance electrical and calcium signaling in plants. *Annu Rev Plant Biol* **67**, 287–307 (2016).
22. Franceschi, V. R. & Nakata, P. A. Calcium oxalate in plants: formation and function. *Annu Rev Plant Biol* **56**, 41–71 (2005).
23. De Silva, D. L., Mansfield, T. A. & McAinsh, M. R. Changes in stomatal behaviour in the calcicole *Leontodon hispidus* due to the disruption by ozone of the regulation of apoplastic Ca<sup>2+</sup> by trichomes. *Planta* **214**, 158–162 (2001).
24. Wang, Y. *et al.* CNGC2 Is a Ca<sup>2+</sup> influx channel that prevents accumulation of apoplastic Ca<sup>2+</sup> in the leaf. *Plant Physiol* **173**, 1342–1354 (2017).
25. Han, M. H. *et al.* Flavonoids Isolated from Flowers of *Lonicera japonica* Thunb. Inhibit Inflammatory Responses in BV2 Microglial Cells by Suppressing TNF- $\alpha$  and IL- $\beta$  Through PI3K/Akt/NF- $\kappa$ B Signaling Pathways. *Phytother Res* **11**, 1824–1832 (2016).
26. Kong, D. *et al.* A comparative study of the dynamic accumulation of polyphenol components and the changes in their antioxidant activities in diploid and tetraploid *Lonicera japonica*. *Plant Physiol Biochem* **112**, 87–96 (2017).
27. Park, K. I. *et al.* Polyphenolic compounds from Korean *Lonicera japonica* Thunb. induces apoptosis via AKT and caspase cascade activation in A549 cells. *Oncol Lett* **4**, 2521–2530 (2017).
28. Wang, Y. *et al.* Validation of Suitable Reference Genes for Assessing Gene Expression of MicroRNAs in *Lonicera japonica*. *Front Plant Sci* **7**, 1101 (2016).
29. Wu, J. *et al.* Flavone synthases from *Lonicera japonica* and *L. macranthoides* reveal differential flavone accumulation. *Sci Rep* **6**, 19245 (2016).
30. Yuan, Y. *et al.* Genetic variation and metabolic pathway intricacy govern the active compound content and quality of the Chinese medicinal plant *Lonicera japonica* thunb. *BMC Genomics* **13**, 195 (2012).
31. Zha, L. *et al.* DNA Methylation Influences Chlorogenic Acid Biosynthesis in *Lonicera japonica* by Mediating LjbZIP8 to Regulate Phenylalanine Ammonia-Lyase 2 Expression. *Front Plant Sci* **8**, 1178 (2017).
32. Zhu, W. *et al.* Proteomic Analysis of *Lonicera japonica* Thunb. Immature Flower Buds Using Combinatorial Peptide Ligand Libraries and Polyethylene Glycol Fractionation. *J Proteome Res* **1**, 166–81 (2016).
33. Zhu, W. *et al.* Variations of metabolites and proteome in *Lonicera japonica* Thunb. buds and flowers under UV radiation. *Biochim Biophys Acta* **4**, 404–413 (2017).
34. Wu, G. *et al.* *Lonicera confusa* has an anatomical mechanism to respond to calcium-rich environment. *Plant Soil* **338**, 343–353 (2011).
35. Yuan, D. X. On the karst ecosystem. *Acta Geol Sin-Engl* **75**, 336–338 (2001).
36. Wu, G. *et al.* Metal Contents in Leaves at Different Developing Phase of Two *Flos lonicerarum* Plants in Karst Region. *Journal of Agro-Environment Science* **26**, 746–749 (2007).
37. Hu, X. *et al.* Calcium-calmodulin is required for abscisic acid-induced antioxidant defense and functions both upstream and downstream of H<sub>2</sub>O<sub>2</sub> production in leaves of maize (*Zea mays*) plants. *New Phytol* **173**, 27–38 (2007).
38. Zhang, L. *et al.* Different Gene Expression Patterns between Leaves and Flowers in *Lonicera japonica* Revealed by Transcriptome Analysis. *Front Plant Sci* **7**, 637 (2016).
39. Maere, S., Heymans, K. & Kuiper, M. BiNGO: a Cytoscape plugin to assess overrepresentation of gene ontology categories in biological networks. *Bioinformatics* **21**, 3448–3449, <https://doi.org/10.1093/bioinformatics/bti551> (2005).
40. Gilliham, M. *et al.* Calcium delivery and storage in plant leaves: exploring the link with water flow. *J Exp Bot* **62**, 2233–2250 (2011).
41. Conn, S. J. *et al.* Cell-specific vacuolar calcium storage mediated by CAX1 regulates apoplastic calcium concentration, gas exchange, and plant productivity in *Arabidopsis*. *Plant Cell* **23**, 240–257 (2011).
42. Webb, A. A. *et al.* The role of calcium in ABA-induced gene expression and stomatal movements. *Plant J* **26**, 351–362 (2001).
43. Dayod, M. *et al.* Calcium storage in plants and the implications for calcium biofortification. *Protoplasma* **247**, 215–231 (2010).
44. Lu, S. X. & Hrabak, E. M. An *Arabidopsis* calcium-dependent protein kinase is associated with the endoplasmic reticulum. *Plant Physiol* **128**, 1008–1021 (2002).
45. Cheong, Y. H. *et al.* CBL1, a calcium sensor that differentially regulates salt, drought, and cold responses in *Arabidopsis*. *Plant Cell* **15**, 1833–1845 (2003).
46. Conn, S. & Gilliham, M. Comparative physiology of elemental distributions in plants. *Ann Bot* **105**, 1081–1102 (2010).
47. Baxter, I. *et al.* Genomic comparison of P-type ATPase ion pumps in *Arabidopsis* and rice. *Plant Physiol* **132**, 618–628 (2003).
48. Cheng, N. H. & Hirschi, K. D. Cloning and characterization of CXIP1, a novel PICOT domain-containing *Arabidopsis* protein that associates with CAX1. *J Biol Chem* **278**, 6503–6509 (2003).
49. Zhang, W. H., Rengel, Z. & Kuo, J. Determination of intracellular Ca<sup>2+</sup> in cells of intact wheat roots: loading of acetoxymethyl ester of Fluo-3 under low temperature. *Plant J* **15**, 147–151 (1998).
50. Slocum, R. & Roux, S. An improved method for the subcellular localization of calcium using a modification of the antiminate precipitation technique. *J Histochem Cytochem* **30**, 617–629 (1982).
51. Wu, G. *et al.* Characterization and molecular interpretation of the photosynthetic traits of *Lonicera confusa* in Karst environment. *PLoS One* **9**, e100703 (2014).

## Acknowledgements

The research was supported by the funds of Hubei Collaborative Innovation Center for the Characteristic Resources Exploitation of Dabie Mountains (2015TD03), the National Natural Science Foundation of China (31270373, 31540083) and New Century Talents Support Program by the Ministry of Education of China (NCET110172). The authors are grateful to Analytical and Testing Center of Huazhong University of Science and Technology for their technical assistance.

## Author Contributions

M.L. and L.B. designed the research. W.J. performed the experiments and analyzed the data. Y.L., C.F., J.X. and B.W. provided the reagents, materials and helped to analyze the data. L.Z. wrote the paper. M.L. revised the paper.

## Additional Information

**Supplementary information** accompanies this paper at <https://doi.org/10.1038/s41598-018-25611-5>.

**Competing Interests:** The authors declare no competing interests.

**Publisher's note:** Springer Nature remains neutral with regard to jurisdictional claims in published maps and institutional affiliations.



**Open Access** This article is licensed under a Creative Commons Attribution 4.0 International License, which permits use, sharing, adaptation, distribution and reproduction in any medium or format, as long as you give appropriate credit to the original author(s) and the source, provide a link to the Creative Commons license, and indicate if changes were made. The images or other third party material in this article are included in the article's Creative Commons license, unless indicated otherwise in a credit line to the material. If material is not included in the article's Creative Commons license and your intended use is not permitted by statutory regulation or exceeds the permitted use, you will need to obtain permission directly from the copyright holder. To view a copy of this license, visit <http://creativecommons.org/licenses/by/4.0/>.

© The Author(s) 2018